# Comparison of linear and RISTRA cavities for a 1064 nm pumped $CdSiP_2$ OPO

Georgi Marchev[a)], Aleksey Tyazhev[a)], Georg Stöppler[b)], Marc Eichhorn[b)], Peter Schunemann[c)], Valentin Petrov[a)]

[a]Max-Born-Institute for Nonlinear Optics and Ultrafast Spectroscopy, 2A Max-Born-Str., D-12489 Berlin, Germany;
[b]French–German Research Institute of Saint-Louis (ISL), 5 rue du Général Cassagnou, BP 70034, 68301 Saint Louis Cedex, France;
[c]BAE Systems, Inc., MER15-1813, P.O. Box 868, Nashua, NH 03061-0868, USA

## ABSTRACT

The beam quality of the idler output of a 1064 nm pumped OPO based on $CdSiP_2$ is compared for linear and Rotated Image Singly-Resonant Twisted RectAngle (RISTRA) cavities. For similar mirrors and cavity round trip times the RISTRA cavity yielded 64 μJ of idler energy (6.4 mW of average power at 100 Hz) compared to 34 μJ with the linear cavity, at a pump level of 21.5 mJ, roughly two times above threshold. The RISTRA cavity generated a somewhat smoother idler beam spatial profile (characterized by moving a knife-edge) and the intensity in the focus of a 10-cm lens was about 50% higher.

Key words: optical parametric oscillators; mid-infrared; RISTRA; $CdSiP_2$

## 1. INTRODUCTION

Recently, we demonsrated that the new nonlinear crystal $CdSiP_2$ (CSP) is a perfect candidate for frequency conversion to the mid-IR spectral range around 6.2 μm by pumping an optical parametric oscillator (OPO) at 1064 nm in a non-critical phase-matching configuration.[1] This is due to a great extent to the exceptionally high effective nonlinearity of CSP, $d_{eff}=d_{36}=84.5$ pm/V.[2] In fact, we could show later that moderate heating of the crystal is a feasible way to achieve idler wavelengths at 6.45 μm, interesting for medical applications (minimally invasive surgery), still preserving the non-critical condition in type-I (oo-e) interation.[3] Regarding the eventual fiber coupling of the 6.45 μm radiation the demands on the OPO beam quality are not very high. Nevertheless, a good OPO efficiency is coupled to both, the beam quality of the pump and the one of the OPO signal and idler beams. This will be difficult in a standard two-mirror OPO cavity associated with a large Fresnel number $\mathcal{F}=D^2/\lambda L$ due to the short OPO cavity length $L$ and the large beam diameter $D$ needed to avoid optical damage ($\lambda$ denotes the resonated wave). The problem is quite critical especially for CSP since the combination of high effective nonlinearity and residual losses at the pump and signal wavelengths (these losses are not intrinsic to CSP but have still to be suppressed in an improved growth process) naturally leads to selection of shorter OPO active elements (of the order of 1 cm) while power/energy scaling would require large beam diameters to avoid not only surface damage but also saturation effects. Pumping with shorter pulses on the other hand also helps reaching the OPO threshold before optical damage occurs (since the latter is fluence dependent) and cavities should be as short as possible to ensure sufficient number of round trips.

Thus, a special OPO cavity geometry is needed for optimum performance. The design of such a cavity geometry has been shortly described as a non-planar four-mirror cavity with image-rotation.[4] The image rotation, working in conjunction with crystal birefringence, significantly improves the spatial quality of the beam even at large pump spot diameters.[4,5] The special OPO cavity design called RISTRA (Rotated Image Singly-Resonant Twisted RectAngle) makes an intracavity image rotation, the pumped region is thus better utilized by the oscillating signal and a much more uniform phase is obtained across the beam, leading to a more symmetric beam shape. The principle of image rotation works in conjunction with angle critical birefringent phase-matching to increase phase front correlation across the beam profile.

Nonlinear Frequency Generation and Conversion: Materials, Devices, and Applications XI, edited by Konstantin L. Vodopyanov, Proc. of SPIE Vol. 8240, 82400E · © 2012 SPIE · CCC code: 0277-786X/12/$18 · doi: 10.1117/12.907436

With this technique the beam is spatially averaged. Image rotation is particularly effective for improving beam quality in high energy OPOs, where the ratio of beam diameter to cavity length results in a cavity Fresnel number that can be intentionally large.The detailed description of this principle, which has already been verified experimentally, can be found in the literature.[4-6]

The RISTRA concept is not wavelength dependent and thus suitable for generation of idler wavelengths at 6.45 µm. It was originally implemented with single-frequency operation and type-II interaction, yielding optimum performance with flat-top pump (and seed) spatial profiles. However, type-I interaction and broadband unseeded operation with $ZnGeP_2$ pumped at 2.05 µm with a Gaussian spatial distribution showed also very promising results in terms of conversion effciency and signal beam (at 3.4 µm) spatial quality.[6] Unfortunately no information on the idler output was presented in this paper.

In the present work we investigated the feasibility of the RISTRA concept for a 1064 nm pumped OPO based on CSP. We compared the idler beam quality for similar mirrors and cavity round trip times using a RISTRA cavity and a linear cavity. Type-I interaction is used for CSP and the RISTRA concept is tested for the fist time under 90°-phase-matcing.

## 2. EXPERIMENTAL SET-UP

The CSP sample used in the present study (Fig. 1a) was cut at $\theta$=90°, $\varphi$=45° and had a length of 9.5 mm. Its aperture was 6 mm (along the ***c***-axis) × 6.75 mm. The crystal ***c***-axis and the pump polarization were in the horizontal plane (oo-e interaction). The residual losses measured for the relevant polarizations (e for the pump and o for the signal and idler) are 0.185 $cm^{-1}$ at 1064 nm, 0.114 $cm^{-1}$ at 1.3 µm, and 0.014 $cm^{-1}$ at 6.2-6.4 µm. Both faces were AR-coated for the three wavelengths (pump, signal, and idler) and the 8-layer coating (TwinStar) had average reflectivity per surface of ~0.35% at 1064 nm, ~0.4% at 1275 nm, and ~0.8% at 6.4 µm. A measurement prior to the OPO experiment gave a transmission of 77% at 1064 nm for the AR-coated sample.

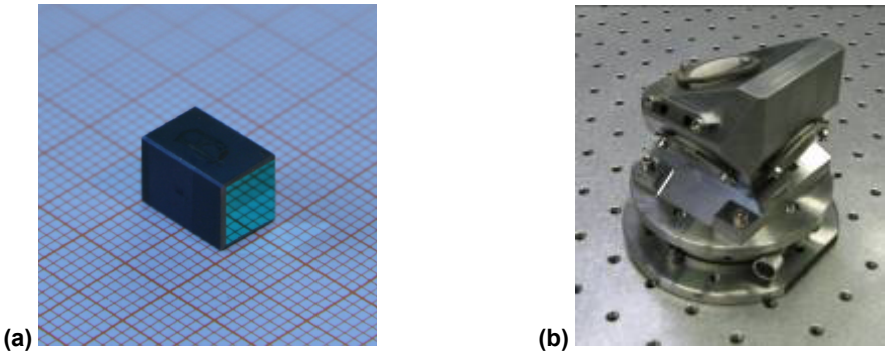


Fig. 1. Photographs of the AR-coated CSP sample (a) and the RISTRA OPO cavity (b).

The RISTRA cavity is shown in Fig. 1b. It contained an input coupler, HT at 1064 nm and 6125 nm for the pump and idler and HR at 1288 nm for the signal (in all cases for an angle of incidence of ~32.8°), and an output coupler, with similar specifications at the pump and idler wavelengths but with partial reflectivity for the signal wavelength (78% for s-polarization and 72% for p-polarization at the same angle of incidence of ~32.8°). The mirrors were on 1" diameter ZnSe substrates, 1/8" thick (TwinStar) and their rear surfaces were AR-coated for the pump and idler radiation. The remaining two RISTRA bending mirrors were of the same kind as the input coupler. Thus only the signal is resonated in the cavity and the pump beam passes just once through the CSP crystal. The physical RISTRA cavity length was 128 mm which corresponds to an optical length of $L$~147 mm.

The physical cavity length of the linear OPO cavity was 55 mm, so that a double pass through the CSP crystal corresponds to an optical length of $L$=148 mm, almost the same as for the RISTRA cavity. The linear cavity was also

pumped in single pass and only the signal was resonated. As an input mirror we used the same input coupler as for the RISTRA cavity since we established that it is HR for the signal wavelength also at normal incidence and the transmission at the pump wavelength was still sufficiently high. As an output coupler for the linear cavity we used a 1" diameter dielectric mirror on a ZnS substrate (TwinStar) with 70% reflectivity for the signal wavelength, HT and with AR-coatings on the rear surface for the pump and idler wavelengths.

The pump source was a diode-pumped and electro-optically Q-switched Nd:YAG laser (Innolas), optimized for a repetition rate of 100 Hz. According to the specifications, its linewidth amounts to 1 $cm^{-1}$, $M^2$ is ~4 and the divergence is <0.5 mrad. The laser generated 100 mJ, 14 ns (FWHM) pulses with an average power of 10 W. The measured energy stability was +/-1%. The pump laser was protected by a Faraday isolator and the separation to the OPO was large enough to avoid feedback during the Q-switching process. A combination of a half-wave plate and a polarizer served to adjust the pump energy. The pump beam exhibited quasi-Gaussian spatial profile with $1/e^2$ diameters of $2w_X$ = 5.5 mm and $2w_Y$ = 4.2 mm in the horizontal and vertical planes, respectively. After expanding the beam with a telescope consisting of two lenses (-40 mm and +75 mm), these diameters increased to $2w_X$ = 9.8 mm and $2w_Y$ = 8.1 mm, respectively. The pump beam was then passed through a circular aperture to obtain a quasi-flat top spatial distribution. The spatial profile after the aperture was characterized by a CCD camera (Fig. 2a shows an image and two cross sections) and by the knife-edge method, calculating the first derivative of the measured average power dependence as a function of the horizontal coordinate (Fig. 2b). The latter measurement provides a rather smooth distribution but this is due to the integration of the power in the vertical direction. The spatial distribution is globally flat but locally modulated by diffraction rings. As can be seen from Fig. 2, the obtained pump beam size is optimum for filling the available CSP crystal aperture. The Fresnel number $\mathcal{F}=D^2/\lambda L$ is ~100. Note that this number can be roughly 10 times higher in a short cavity OPO as the one used in the first experiment with CSP.[1]

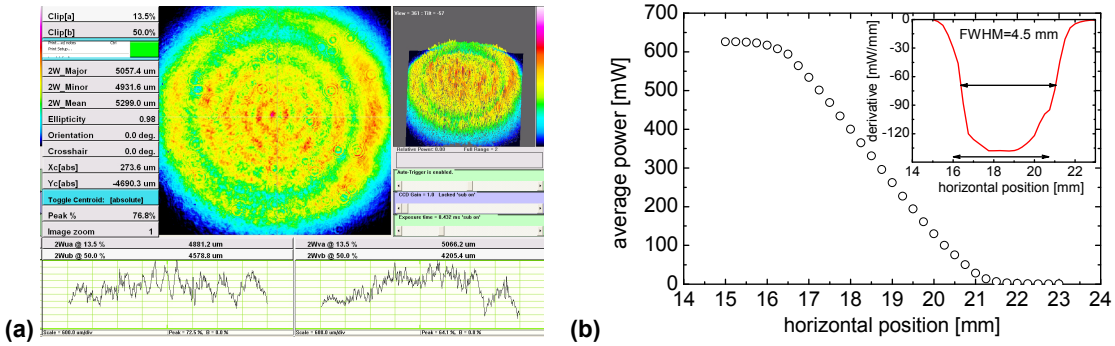


Fig. 2. CCD image of the pump spatial profile after the aperture (a) and measurement by the knife-edge method (b).

Since the input couplers had different transmission at the pump wavelength, to compare the two cavities we studied the dependence on the pump energy incident on the CSP crystal. The maximum available pump energy incident on the CSP crystal was about 21.5 mJ in the case of the linear cavity, hence, we set the same upper limit also for the RISTRA cavity. The calculated pump intensity values correspond to the axial pump intensity, calculated from the measured incident energy by taking into account the aperture transmission (~1/2.7), the quasi-Gaussian beam spatial profile in front of the aperture, and the pump pulse duration of 14 ns.

## 3. RESULTS AND DISCUSSION

Figure 3 shows the dependence of the idler output energy on the incident pump energy for the RISTRA and linear OPO cavities. The RISTRA pump threshold was 10.5 mJ corresponding to on-axis pump intensity of 6.4 $MW/cm^2$. The RISTRA cavity yielded a maximum idler pulse energy of 64 µJ (6.4 mW of average power at 100 Hz) compared to 34 µJ with the linear cavity, at a pump level of 21.5 mJ, in both cases roughly two times above the OPO threshold.

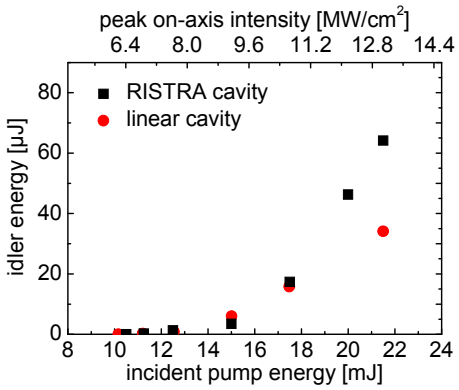


Fig. 3. Idler pulse energy versus pump energy incident on the CSP crystal.

At first we evaluated the idler beam diameter by the knife-edge method using a 10-cm focal length $BaF_2$ lens positioned at 50 cm from the OPO output coupler (Fig. 4a). The beam waists obtained were similar for the linear and RISTRA cavities but the beam diameter on the lens was roughly two times smaller in the case of the RISTRA cavity due to the smaller divergence in this case. For a fair comparison we increased then the separation of the lens from the output coupler to 100 cm and the corresponding results are shown in Fig. 4b. The idler beam diameter at the position of the lens corresponds to abscissa zero. The idler beam diameter just after the RISTRA cavity was about 4 mm.

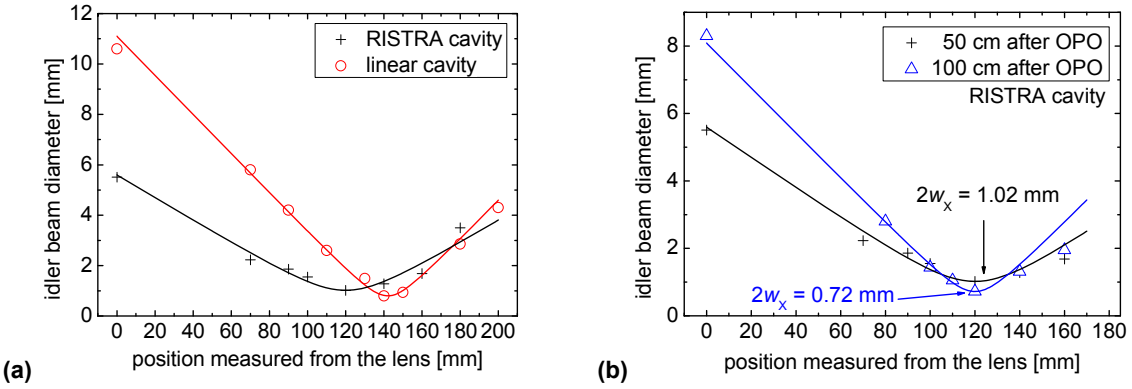


Fig. 4. Idler beam horizontal diameter dependence on the position after a 10-cm focusing lens. Comparison between RISTRA and linear cavity with the lens at 50 cm from the OPO output coupler (a) and RISTRA cavity idler focusability with the 10-cm lens positioned at 50 and 100 cm from the OPO output coupler (b).

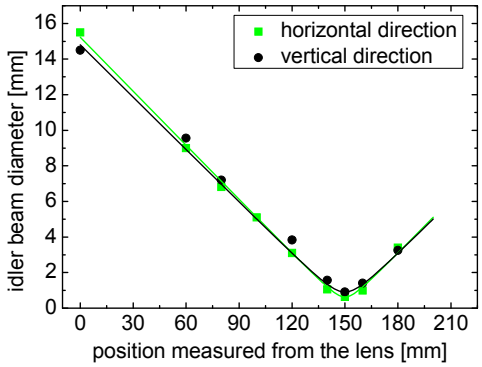


Fig. 5. Idler beam diameter dependence measured with fully illuminated focusing lens with focal length of 10 cm.

To obtain minimum beam diameter in the focal spot, we expanded the idler beam after the RISTRA OPO to fill almost completely the aperture of the 10-cm $BaF_2$ focusing lens. The idler beam diameter on the lens amounted to ~15 mm (FWHM). The beam diameters in the horizontal and vertical planes were measured at several positions after the lens. The results are plotted in Fig. 5. The minimum obtained focal diameters were $2w_X$=630 μm and $2w_Y$=910 μm, in the horizontal and vertical directions, respectively.

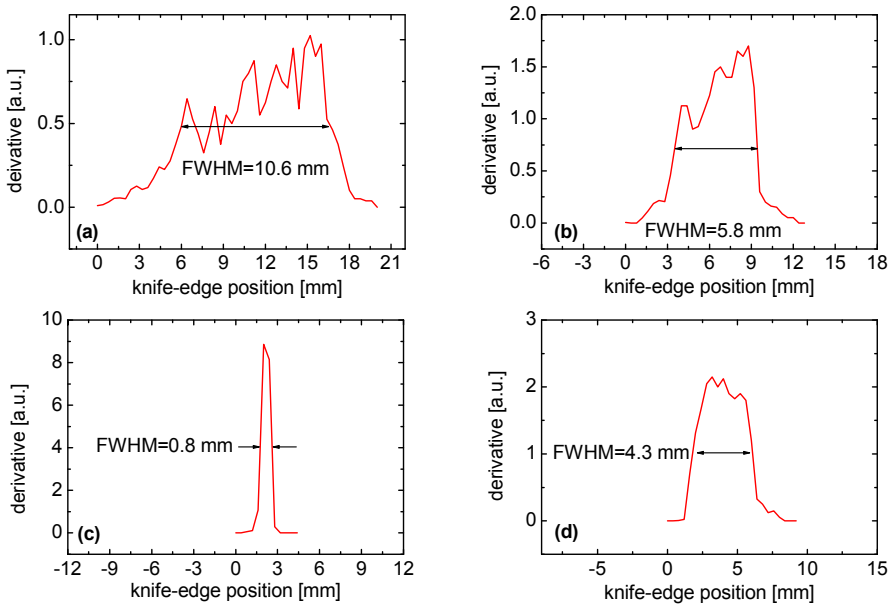


Fig. 6. Idler beam profile and diameters in horizontal direction at several points after the 10-cm $BaF_2$ focusing lens, positioned 50 cm from the output coupler of the linear OPO cavity. (a) on the lens, (b) 7 cm after the lens, (c) 14 cm after the lens (focal point), and (d) 20 cm after the lens.

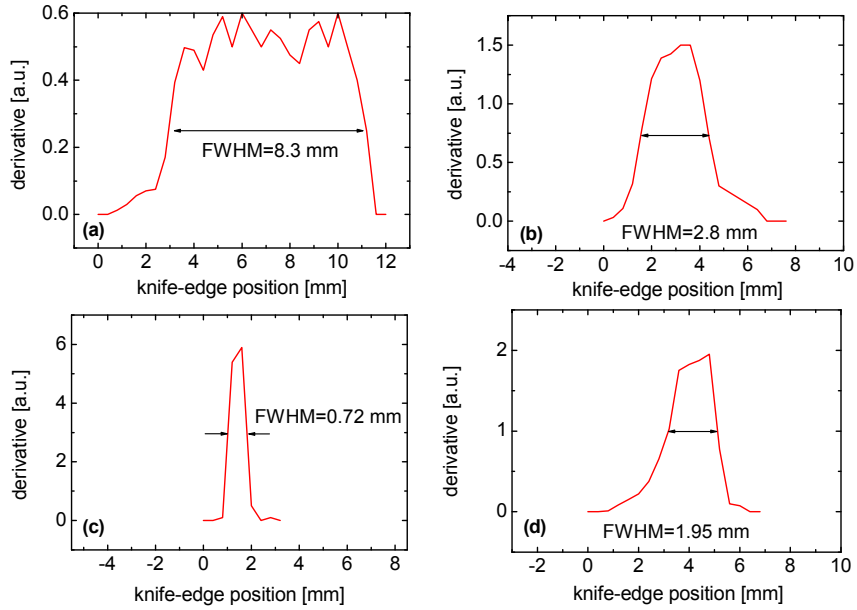


Fig. 7. Idler beam profile and diameters in horizontal direction at several points after the 10-cm $BaF_2$ focusing lens, positioned 100 cm from the output coupler of the RISTRA OPO cavity. (a) on the lens, (b) 8 cm after the lens, (c) 12 cm after the lens (focal point), and (d) 16 cm after the lens.

In Figs. 6 and 7 we compare the idler beam profiles from both cavity configurations for the same beam diameter on the focusing lens. Figure 6 refers to the linear cavity with the 10-cm focusing lens at 50 cm from the output coupler and Fig. 7 refers to the RISTRA cavity with the 10-cm focusing lens at 100 cm from the output coupler It can be seen that the RISTRA cavity produces slightly more uniform idler beam spatial profile.

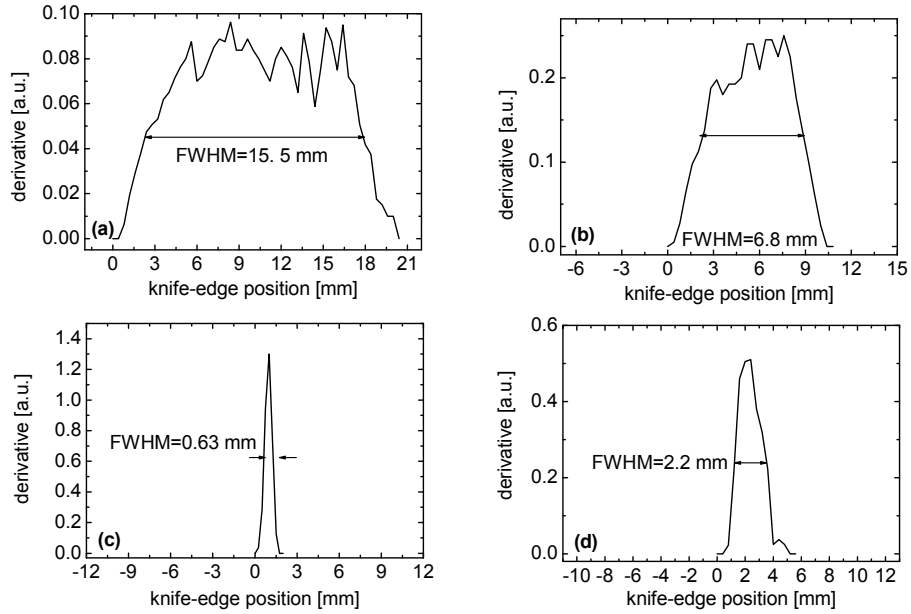


Fig. 8. RISTRA OPO idler beam profile and diameter in the horizontal direction at several points after the fully illuminated 10-cm $BaF_2$ focusing lens. (a) on the lens, (b) 8 cm after the lens, (c) 15 cm after the lens (focal spot), and (d) 18 cm after the lens.

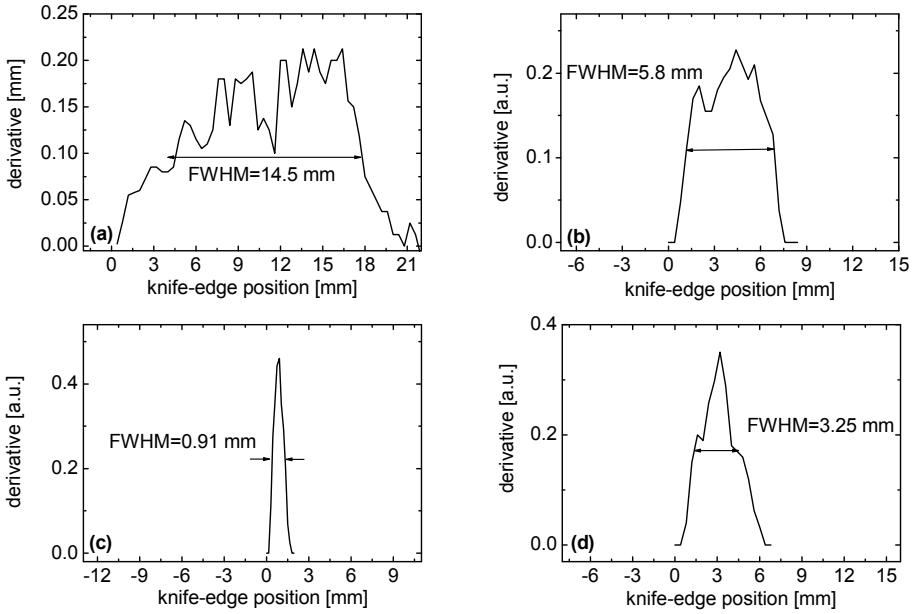


Fig. 9. RISTRA OPO idler beam profile and diameter in the vertical direction at several points after the fully illuminated 10-cm $BaF_2$ focusing lens. (a) on the lens, (b) 8 cm after the lens, (c) 15 cm after the lens (focal spot), and (d) 18 cm after the lens.

Finally, in Figs. 8 and 9 we have plotted the idler beam profiles from the RISTRA cavity with the beam expanded to fully illuminate the 10-cm focusing lens. These plots correspond to the data in Fig. 5. Comparing the focal spot sizes achievable with the two cavities, only about 50% enhancement in the maximum achievable intensity is observed in the case of the RISTRA cavity.

## 4. CONCLUSION

In conclusion, we compared the performance of RISTRA and linear cavities for a 1064 nm pumped OPO based on CSP. The pump source was multimode and broadband with quasi-flat top spatial distribution. Only the non-resonated idler output beam quality was studied. The nonlinear interaction was of type-I (oo-e). The improvement in the spatial quality of the idler beam employing the RISTRA cavity was marginal in the low conversion limit studied (pump exceeding the threshold not more than twice) although the conversion efficiency was somewhat better. Since the RISTRA concept has previously been proven to be useful under similar conditions with type-I interaction, the absence of angle birefringence in non-critical 90° phase-matching is considered to be the main reason for the marginal spatial quality improvement observed in the present study.

## ACKNOWLEDGMENTS

The research leading to these results has received funding from the European Community's Seventh Framework Programme FP7/2007-2011 under grant agreement n°224042.

## REFERENCES

[1] V. Petrov, P. G. Schunemann, K. T. Zawilski, T. M. Pollak, "Noncritical singly resonant optical parametric oscillator operation near 6.2 μm based on a $CdSiP_2$ crystal pumped at 1064 nm," Opt. Lett. **34**, 2399-2401 (2009).

[2] V. Kemlin, B. Boulanger, V. Petrov, P. Segonds, B. Ménaert, P. G. Schunneman, K. T. Zawilski, "Nonlinear, dispersive, and phase-matching properties of the chalcopyrite $CdSiP_2$," Opt. Mater. Express **1**, 1292-1300 (2011).

[3] V. Petrov, G. Marchev, P. G. Schunemann, A. Tyazhev, K. T. Zawilski, and T. M. Pollak, "Subnanosecond, 1 kHz, temperature-tuned, noncritical mid-infrared optical parametric oscillator based on $CdSiP_2$ crystal pumped at 1064 nm," Opt. Lett. **35**, 1230-1232 (2010).

[4] A. V. Smith and D. J. Armstrong, "Nanosecond optical parametric oscillator with 90° image rotation: design and performance," J. Opt. Soc. Am. B **19**, 1801–1814 (2002).

[5] D. J. Armstrong and A. V. Smith, "All solid-state high-efficiency tunable UV source for airborne or satellite-based ozone DIAL systems," IEEE J. Sel. Top. Quantum Electron. **1**3, 721-731 (2007).

[6] A. Dergachev, D. Armstrong, A. Smith, T. Drake, M. Dubois, "3.4-μm ZGP RISTRA nanosecond optical parametric oscillator pumped by a 2.05-μm Ho:YLF MOPA system," Opt. Express **15**, 14404-14413 (2007).